LT Scaling in Depleted Quantum Spin Ladders

S. Galeski,[1,2,*] K. Yu. Povarov,[1] D. Blosser,[1] S. Gvasaliya,[1] R. Wawrzynczak,[2,3]
J. Ollivier,[3] J. Gooth,[2] and A. Zheludev[1,†]
[1]*Laboratory for Solid State Physics, ETH Zürich, 8093 Zürich, Switzerland*
[2]*Max Planck Institute for Chemical Physics of Solids, Nöthnitzer Strasse 40,01187 Dresden, Germany*
[3]*Institut Laue-Langevin, 6 rue Jules Horowitz, 38042 Grenoble, France*

(Received 15 November 2021; revised 2 May 2022; accepted 10 May 2022; published 10 June 2022)

Using a combination of neutron scattering, calorimetry, quantum Monte Carlo simulations, and analytic results we uncover confinement effects in depleted, partially magnetized quantum spin ladders. We show that introducing nonmagnetic impurities into magnetized spin ladders leads to the emergence of a new characteristic length L in the otherwise scale-free Tomonaga-Luttinger liquid (serving as the effective low-energy model). This results in universal LT scaling of staggered susceptibilities. Comparison of simulation results with experimental phase diagrams of prototypical spin ladder compounds bis(2,3-dimethylpyridinium)tetrabromocuprate(II) (DIMPY) and bis(piperidinium)tetrabromocuprate(II) (BPCB) yields excellent agreement.

DOI: 10.1103/PhysRevLett.128.237201

Understanding the interplay of electron correlation and disorder is one of the central problems of condensed matter physics. The influence of disorder becomes crucial in one dimension where the nontrivial topology does not allow for quasiparticles to avoid even the smallest defects [1]. The impact of such interaction can be especially dramatic in gapless many-body 1D systems realizing a quantum critical Tomonaga-Luttinger liquid (TLL)—a one-dimensional analog of the celebrated Fermi liquid [1–4]. Similarly to the latter, the TLL is characterized by the analog of Fermi velocity v that sets the energy scale (conveniently expressed in units such as Kelvin), and additional exponent K reflecting the strength and type of interactions in the system.

A paradigmatic model for the study of the TLL physics is the simple $S = 1/2$ Heisenberg chain. Recent studies of site disorder in spin chain materials have shown that introduction of defects into the chain lattice effectively divides the liquid into finite pieces [5,6]. Such segmentation has a profound effect on the low temperature properties of the TLL: the pure system, being in a quantum critical state is characterized by only a single energy scale—temperature T. Introduction of defects imposes a novel scale: the average distance between defects L and leads to discretization of the TLL energy levels with a v/L step [see Fig. 1(a)]. This in turn leads to the replacement of the original T universality by a new LT universality: all dynamic and thermodynamic observables become functions of the product LT only [6–8]. However, for the general anisotropic XXZ case such theoretical studies were performed only in the $T = 0$ limit so far [9].

A central question in the study of defects in low-dimensional quantum magnets is whether the LT scaling is a truly universal property of disordered TLLs, even when defects do not break the liquid's continuity and for arbitrary TLL exponent K. The simplest realistic model allowing for the study of this problem is the depleted Heisenberg $S = 1/2$ ladder. Unlike the spin chain, it offers a much less restrictive geometry since removing one spin from the lattice does not break the ladder continuity, as shown Fig. 1. In addition, different interaction parameters K can be achieved in ladders with different rung and leg exchange coupling ratios $J_\perp/J_\parallel$, with strong leg ladders displaying attractive and strong rung ladders repulsive interactions [10]. This K exponent is also tunable by the magnetic field, and is usually found from numeric simulations for a given system [11]. Thus, the depleted spin ladder magnets open up an avenue to explore the "dirty TLL" physics in the most generic, controlled, and tunable way.

In this Letter we experimentally and theoretically study the effect of spin depletion on two organometallic spin ladder materials: BPCB [12–15] and DIMPY [16–19]. Both of these materials are well-established realizations of the $S = 1/2$ Heisenberg ladder Hamiltonian and harbor an attractive (DIMPY) and repulsive (BPCB) TLL when magnetized [10,12,16]. The most relevant parameters of the materials are given in Table I [20]. Using inelastic neutron scattering we experimentally confirm the applicability of the depleted ladder model to Zn^{2+} ($S = 0$)-substituted

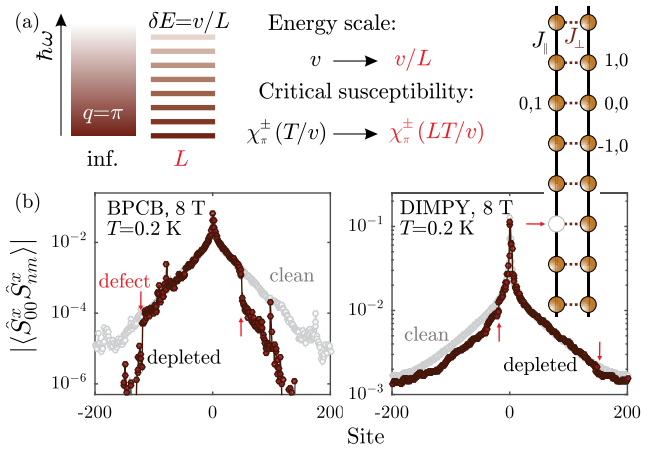

FIG. 1. (a) Origin of LT scaling in Tomonaga-Luttinger liquids. Finite-size effect results in equidistant discretization of the energy spectrum at critical wave vector and in effect to suppression of corresponding susceptibility. (b) A QMC simulation of the transverse two-spin correlator in a pure and depleted 400-site magnetized DIMPY and BPCB spin ladders. The two randomly placed defects in the ladder (shown by red arrows) are partially "transparent" to correlations.

BPCB. Using a combination of QMC simulations [21], analytical calculations, and an extensive low temperature heat capacity survey we show that the LT scaling of staggered susceptibilities is a robust, universal property of disordered TLL regardless of the K parameter. Our findings suggest that such scaling persists even if the continuity of TLL remains preserved, a situation inaccessible in the segmented spin chain settings studied before [6–9]. Thus, LT universality appears to be a generic property of "dirty" TLLs.

The samples were grown in house by the thermal gradient [$(C_7H_{10}N)_2Cu_{1-z}Zn_zBr_4$ DIMPY] and solvent evaporation [$(C_5H_{12}N)_2Cu_{1-z}Zn_zBr_4$ BPCB] methods, similar to the pristine materials [13,17], with replacement of the relevant amount z of $CuBr_2$ by $ZnBr_2$. Both in specific heat and neutron scattering experiments we have used fully deuterated chemicals for growth of BPCB crystals. The Zn^{2+} content in the studied samples was verified using micro x-ray fluorescence chemical analysis and independently cross-checked through comparison of low field magnetization measurements with QMC simulations. The DIMPY samples were already used in the previous study [23].

TABLE I. Magnetic Hamiltonian constants of BPCB [12] and DIMPY [16] for rung, leg, and interladder interaction and the g factor [13,22] for the relevant field direction. Also the corresponding correlation length ξ in the gapped phase, and TLL parameters at 8 T: Luttinger velocity v, and dimensionless exponent K are given.

	$J_\perp$ (K)	$J_\parallel$ (K)	J' (mK)	$g_{H\|\|a}$	ξ (lat. u.)	v (K)	K
DIMPY	9.5	16.74	75	2.13	6.3	22.04	1.23
BPCB	12.96	3.6	80	2.06	~0.8	3.94	0.93

In a depleted spin ladder, at low magnetic fields the nonmagnetic defects were shown to lead to the emergent clusters of staggered magnetization ("spin islands"), as typical for a gapped system [23,24]. The effect of Zn substitution in DIMPY at low fields has been already thoroughly studied revealing that Zn-doped DIMPY is an excellent realization of a depleted strong leg spin ladder Hamiltonian [23]. However, despite the structural and chemical similarity between BPCB and DIMPY, an assumption that BPCB also realizes a depleted spin ladder Hamiltonian cannot be taken for granted. In order to verify that this is the case we have studied the emergent Zn-induced spin island degrees of freedom in the gapped phase of BPCB. Thanks to the short correlation length in BPCB, these "islands" are expected to exhibit no overlap for low Zn substitution levels and thus behave as uncorrelated paramagnetic impurities and scatter neutrons elastically. Their presence could thus be only detected as a magnetic field induced Zeeman resonance. The localized spin-1/2 degrees of freedom should appear as a nondispersive level, very broad in momentum, centered at $\hbar\omega = g\mu_B\mu_0 H$. A similar kind of Zeeman resonance has been observed in a depleted Haldane material $Y_2BaNi_{1-z}Mg_zO_5$ [25].

In order to test those predictions we have performed an inelastic neutron spectroscopy study of 5 co-aligned $z = 0.02$ BPCB crystals with total mass 0.9 g, at the IN5 time-of-flight spectrometer [26] (ILL, Grenoble) with a split-coil vertical magnet. Figures 2(a) and 2(b) show a comparison between magnetic neutron spectra collected at $T = 60$ mK and in 0 and 2.5 T with the magnetic field applied along the crystals b axis. The data were collected

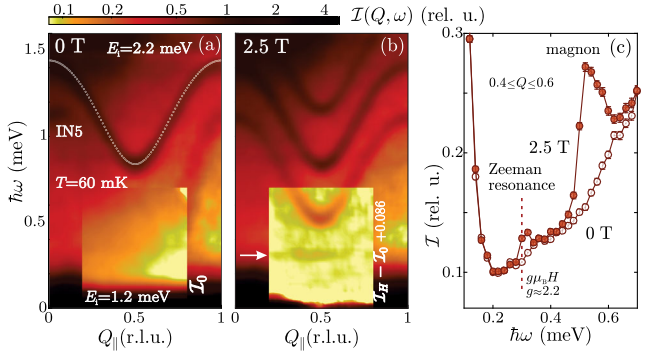

FIG. 2. (a),(b) Magnetic neutron scattering intensity as a function of energy and momentum transfer (along the ladder leg) of depleted BPCB in 0 and 2.5 T. The spectra were taken using an incident neutron energy of 2.2 (in the main panels) and 1.2 meV (in the insets). For 2.5 T case inset shows the background-subtracted intensity; the arrow shows the position of the impurity-related scattering. Dashed line in 0 T panel is the reference magnon dispersion in clean BPCB [28]. (c) Intensity profiles $\mathcal{I}(\omega)$ near $Q_\parallel = 0.5$ r.l.u. Zeeman resonance at 0.3 meV is well visible in the magnetized case.

with 2.2 and 1.2 meV incident energy, then treated with HORACE software [27]. Neutron intensity is shown as a function of energy transfer $\hbar\omega$ and momentum transfer along the leg direction $Q_{\parallel}$. The 0 T spectrum demonstrates that introduction of nonmagnetic defects does not alter the magnon dispersion [28] in any obvious way compared with the pristine material. The dispersion itself is well captured by the strong-rung limit expansion of the spin ladder model [29]. There are no novel low energy features visible over the magnet-related background, justifying the weakly correlated picture of the defects in BPCB, contrasting the case of DIMPY. In contrast, at 2.5 T there appears a clearly distinguishable nondispersive level at 0.3 meV [see Figs. 2(b) and 2(c)]—the expected resonance. The $S = 1$ magnon's dispersion remains unchanged apart from splitting into three branches due to Zeeman effect. This is exactly the behavior one would expect from the depleted spin ladder with the parameters of BPCB. The availability of the "isolated island" analytic solution in the strong-rung limit with short correlations is very helpful, as the numeric simulations of spectral properties are extremely demanding in the presence of disorder. Thus, we are confident that the chemical substitution in both materials functions the same way (merely depleting the spin ladder) and further comparison of critical properties in high magnetic fields would be meaningful.

In magnetic fields strong enough to close the magnon gap, the fate of the spin impurities is expected to change. Above the critical field the spin ladder enters the gapless TLL phase [1,30]. The most distinct difference between TLLs realized in spin chain and magnetized spin ladders is that ladder lattices offer a much less restrictive geometry. Thus it can be expected that introduction of nonmagnetic defects could induce a novel length scale into the problem without sacrificing the TLL continuity. To test if nonmagnetic defects would remain at least partially transparent to spin correlations in magnetized spin ladders we have performed direct quantum Monte Carlo (QMC) simulations of the transverse components of spin-spin correlations $\langle \hat{S}^x_{00} \hat{S}^x_{mn} \rangle$ on two ladder lattices with coupling constants resembling that of our target materials. The calculations have been performed using the `dirloop-sse` algorithm of the ALPS package [21,31]. The results of those calculations displayed in Fig. 1 suggest that as naively expected, spin correlations can propagate along the ladder despite the presence of nonmagnetic defects for both DIMPY and BPCB. Comparing the left and right panel of Fig. 1(b) reveals that defects suppress spin correlations much more efficiently in the case of the repulsive TLL realized in BPCB than in the attractive case of DIMPY.

In order to verify that introduction of defects that do not lead to segmentation of the TLL still leads to the presence of LT scaling in the critical (transverse staggered $\chi^{\pm}_{\pi}$) susceptibility of magnetized depleted ladders, we have performed another series of QMC simulations. Although the ALPS `dirloop-sse` algorithm [21,31] does not give direct access to $\chi^{\pm}_{\pi}$ for magnetized systems, it does allow for the calculation of the static transverse correlation function $\langle S^{+}_{00} S^{-}_{nm} \rangle$. While this quantity is in general not directly related to the susceptibility, in the case of TLL it can be shown that per mol of spins we have

$$\chi^{\pm}_{\pi}(L,T) = \frac{N_A}{k_B} \frac{(g\mu_B)^2}{LT\mathcal{R}(K)} \sum_{n,m,k,l} (-1)^{n-m+k-l} \langle S^{+}_{nk} S^{-}_{ml} \rangle, \quad (1)$$

with $\mathcal{R}(K)$ being a prefactor of the order of 1, that can be analytically derived [20].

Using the QMC results and Eq. (1) we have computed the staggered transverse susceptibility for a series of spin ladder lattices of 10, 20, 50, 100, and 200 rungs with coupling constants resembling those of DIMPY and BPCB, in the 8 T field, and with the boundaries being open. The resulting susceptibilities are plotted in the inset of Fig. 3(a). However, as we can see, the simple $\chi^{\pm}_{\pi}(L,T) \times T$ product does not show apparent scaling as it would in the open boundaries Heisenberg spin chain case with $K = 1/2$ [7]. The temperature-related power law requires a modification here, and we argue that the generalized scaling relation should be [20]

$$\chi^{\pm}_{\pi}(L,T) \propto \left(\frac{T}{v}\right)^{\frac{1}{2K}-2} F_K\left(\frac{LT}{v}\right), \quad (2)$$

with $F_K(x)$ being a K-parametrized single argument function. Once the data are replotted in the respective coordinates [Fig. 3(a)], the presence of scaling (2) in the low-T regime becomes apparent. This is consistent with the power law $T^{1/2K-2}$ for the thermodynamic limit [1]. At higher temperatures the behavior is non-TLL in general and the scaling breaks down.

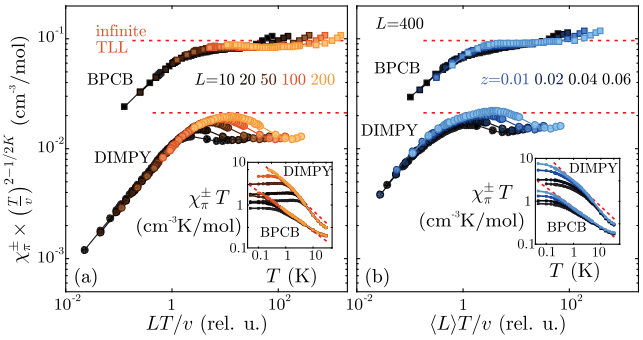

FIG. 3. Comparison of LT/v scaling properties of staggered susceptibilities in finite spin ladder segments and depleted spin ladders. Susceptibility is extracted from QMC data according to Eq. (1); simulations are done at 8 T field for coupling constants of DIMPY and BPCB. (a) Scaling of finite spin ladder segments with open boundary conditions. (b) Scaling of 400 rung diluted spin ladder lattices, here $L = (1 - z/2z - z^2)$ is the average interdefect distance. In both panels the dashed lines show the scaling law expected for the infinite system. Insets shows the unscaled data.

To test the hypothesis that introducing random spin depletion also introduces a new length scale leading to LT scaling we have performed a second set of QMC simulations. Assuming the same coupling parameters and applied magnetic fields we have computed the susceptibilities for both ladder systems with 400 rungs and 1%, 2%, 4%, and 6% spin depletion and averaged over 20 different random impurity distributions. The results of these calculations are displayed in Fig. 3(b). Strikingly despite some differences in overall shape of the curves compared to the finite length pieces, the susceptibilities in "depleted ladders" closely follow the derived scaling law.

These theoretical results would be best confirmed through a direct comparison with measurements of transverse staggered susceptibilities of several samples with a different level of dilution. Although such measurements could be, in principle, carried out using inelastic neutron scattering, in practice it would be a formidable task. Another avenue for testing our QMC results can be provided through testing the ability of our target systems to achieve 3D ordering. One of the most spectacular ways spin depletion influences low temperature properties of quasi-1D magnets is through altering their ordering capabilities: in ultrapure site diluted $SrCuO_2$ samples the presence of less than 1% of impurities suppresses Néel ordering beyond experimental detection [6]. The mean field condition for magnetic ordering ties the ordering temperature, critical susceptibility, and the strength of residual 3D couplings J' [30,32,33]:

$$\chi_{\pi}^{\pm}(T_N) = \frac{N_A}{k_B}\frac{(g\mu_B)^2}{J'}. \tag{3}$$

This explains the strong suppression of T_N in depleted spin chains: addition of impurities effectively cuts them, truncating the spin-spin correlations and leading to depression of the relevant susceptibility. Equation (3) defines the critical susceptibility magnitude that triggers long-range ordering. Thus to confirm the validity of our QMC simulations we have calculated the full phase diagram of both pure and depleted DIMPY and BPCB for a direct comparison with experimental phase diagrams obtained from specific heat measurements. We would like to stress that the simulations and measurements are performed away from the critical fields, and so possible Bose-glass related phenomena [34] are not relevant.

The magnetic phase diagrams for all samples were determined through locating the maxima of the specific heat anomalies attributed to 3D ordering via fitting Lorentzian-like peak functions (details are shown in the Supplemental Material [20]). The specific heat measurements were performed in the Quantum Design PPMS dilution refrigerator equipped in a standard specific heat option and a 9 T superconducting magnet. Representative datasets after subtracting the nuclear spin contribution for

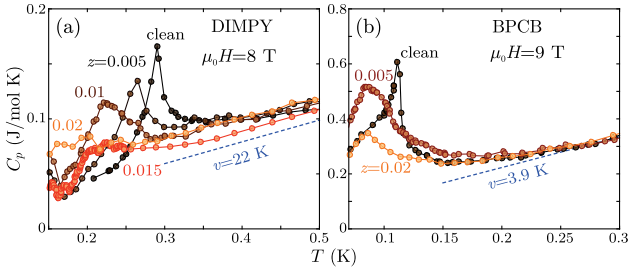

FIG. 4. Comparison of the spin dilution effect on the specific heat anomaly of DIMPY and BPCB measured at 8 and 9 T, respectively. Dashed lines show the expected TLL linear specific heat. Arrows mark the transition temperature.

samples with different Zn substitution level of both DIMPY and BPCB are shown in Fig. 4. Inspection of both datasets reveals that spin depletion apart form quickly suppressing magnetic order additionally leads to broadening of the specific heat anomalies. It was shown that such broadening can be an effect of weak random fields arising due to chemical disorder [35]. Indeed it can be expected that spin depletion of a single ladder not only decreases its staggered transverse susceptibility leading to the depression of T_N but also exerts an effective random field on the neighboring ladders. Interestingly, apart from altering the shape and location of the specific heat anomaly spin depletion seems to have no influence on the high temperature specific heat. This simple observation suggests that although adding nonmagnetic impurities changes the span of correlation functions it does not influence the spinon velocity v as $C_v^{\mathrm{TLL}}(T) = R(\pi/6v)T$. Moreover, previous studies of equal-time correlations scaling in depleted chains [5] suggest that defects do not alter the exponent K either, in agreement with our QMC analysis.

To verify that our QMC procedure is reliable in computing physical properties of the relevant materials we have calculated the longitudinal uniform susceptibility which is a directly observable quantity. For comparison with simulations we have measured the susceptibility of both materials using the PPMS AC-susceptibility option at 8 T. As shown in the inset of Fig. 5(a) the agreement of the QMC result with experiment is excellent confirming the validity of our approach.

The first crucial step in simulating phase diagrams of depleted spin ladders is the determination of the inter ladder coupling constant J'. To do this we have calculated the transverse staggered susceptibility for pure 400 rung systems with periodic boundry conditions and then fitted Eq. (3) to the experimental specic heat data using J' as a fitting parameter, following the procedure of Ref. [16]. As a result we have established the interladder coupling to be 106 and 110 mK for DIMPY and BPCB, respectively, values slightly higher than previously obtained through a combined DMRG and field theory approach. Although estimating T_N for the case of depleted ladders from

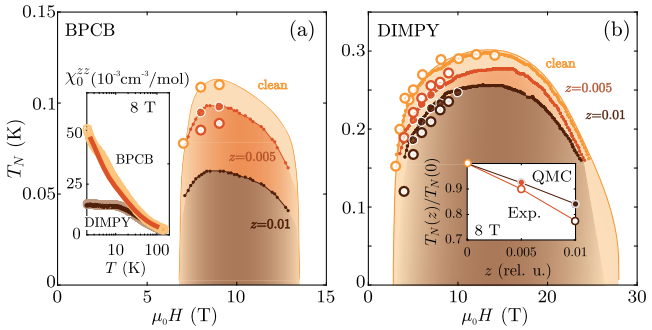

FIG. 5. Comparison of QMC simulation results with experimental phase diagrams obtained from specific heat: large solid circles mark points in the H–T plane where the calculation was performed using 100 random impurity configurations; small circles are the rescaled results with 20 configurations. The large open circles represent results of heat capacity measurements. Thin line for the clean case is the DMRG-based mean field result. (a) The inset shows a comparison of simulated and measured uniform longitudinal magnetic susceptibility per spin of pure DIMPY and BPCB at 8 T (lines are QMC results, symbols are the measured values). (b) The inset shows a comparison of experimental and simulated values of T_N at 8 T.

susceptibility calculations with a similar level of averaging to those used for the scaling analysis to qualitatively reproduce the experimental phase diagram, the predicted phase boundaries showed to be off by over 20% compared to the experimental results. In order to correct for the effect of under averaging we have thus calculated the expected T_N for several fields averaging over 100 random impurity configurations. This allowed us to obtain predictions for T_N with excellent agreement with empirical data.

The final comparison of experimental and calculated phase diagrams is shown in the main panels of Fig. 5. For both materials the QMC result seems to accurately reproduce the phase diagrams for both pure and diluted samples. The excellent predictive power of our QMC calculation confirms that our simulation method can be used to accurately calculate $\chi^{\pm}_{\pi}(T)$ for a range of magnetic fields. This in turn reassures the validity of the LT scaling analysis in depleted spin ladders. Finally, we would like to note that in the case of attractive TLL in DIMPY the ordered phase is much more resistant to defects compared to the case of repulsive TLL in BPCB. This seems to be the experimental consequence of spontaneous defect "healing" in an attractive TLL [36], and is also in line with the direct calculation of (small) correlation suppression in the DIMPY case shown in Fig. 1(b).

Our results combined, with Ref. [23], paint a full picture of the interplay of spin depletion and magnetic fields in spin ladders. At low magnetic fields $H < H_{c1}$ defects introduce packets of localized staggered magnetization that can give rise to a new emergent magnetic system if located densely enough to interact with one another. On the other hand at high fields $H > H_{c1}$ defects truncate the spin-spin correlation introducing a new length scale and introducing the new LT universality even when the TLL is not fully segmented. Those results suggest that the quantum critical state is in general susceptible to adjusting to externally imposed length scales such as disorder. We have verified that the LT scaling generally emerges in the presence of impurities for any degree of continuity and any Luttinger exponent K. Our analysis is expected to be directly transferable to other TLL systems such as nanowires, or the quantum Hall edge states. Another interesting possible application are the 1D disordered quantum magnets with charge degrees of freedom, such as $Sr_{14}Cu_{24}O_{41}$ [37] or $BaFe_2S_3$ [38]. It remains to be verified if our results will hold in these more complex situations.

This work was supported by the Swiss National Science Foundation, Division II. Part of the numerical simulations were performed on the ETH Zürich Euler cluster. We also acknowledge Mr. Jonathan Noky for his assistance in running the calculations on the computing cluster of Max Planck Institute for Chemical Physics of Solids, Dresden. We would like to thank Dr. D. Schmidiger (ETH Zürich) for his involvement at the early stage of the project, Dr. R. Chitra (ETH Zürich) and Dr. Tobias Meng (TU Dresden) for insightful discussions, and Dr. F. Alet (CNRS, Université Paul Sabatier Toulouse) for helpful advice on QMC techniques.

*Corresponding author.
Stanislaw.Galeski@cpfs.mpg.de
†zhelud@ethz.ch

[1] T. Giamarchi, *Quantum Physics in One Dimension* (Oxford University Press, New York, 2003).
[2] I. A. Zaliznyak, A glimpse of a Luttinger liquid, Nat. Mater. **4**, 273 (2005); B. Lake, D. A. Tennant, C. D. Frost, and S. E. Nagler, Quantum criticality and universal scaling of a quantum antiferromagnet, Nat. Mater. **4**, 329 (2005).
[3] B. Lake, A. M. Tsvelik, S. Notbohm, A. D. Tennant, T. G. Perring, M. Reehuis, C. Sekar, G. Krabbes, and B. Büchner, Confinement of fractional quantum number particles in a condensed-matter system, Nat. Phys. **6**, 50 (2010).
[4] A. Zheludev, Quantum critical dynamics and scaling in one-dimensional antiferromagnets, J. Exp. Theor. Phys. **131**, 34 (2020).
[5] G. Simutis, S. Gvasaliya, M. Månsson, A. L. Chernyshev, A. Mohan, S. Singh, C. Hess, A. T. Savici, A. I. Kolesnikov, A. Piovano, T. Perring, I. Zaliznyak, B. Büchner, and A. Zheludev, Spin Pseudogap in Ni-Doped $SrCuO_2$, Phys. Rev. Lett. **111**, 067204 (2013); G. Simutis, S. Gvasaliya, N. S. Beesetty, T. Yoshida, J. Robert, S. Petit, A. I. Kolesnikov, M. B. Stone, F. Bourdarot, H. C. Walker, D. T. Adroja, O. Sobolev, C. Hess, T. Masuda, A. Revcolevschi, B. Büchner, and A. Zheludev, Spin pseudogap in the $S = \frac{1}{2}$ chain material Sr_2CuO_3 with impurities, Phys. Rev. B **95**, 054409 (2017).
[6] G. Simutis, M. Thede, R. Saint-Martin, A. Mohan, C. Baines, Z. Guguchia, R. Khasanov, C. Hess, A. Revcolevschi, B. Büchner, and A. Zheludev, Magnetic ordering in the ultrapure

site-diluted spin chain materials $SrCu_{1-x}Ni_xO_2$, Phys. Rev. B **93**, 214430 (2016).

[7] S. Eggert, I. Affleck, and M. D. P. Horton, Néel Order in Doped Quasi-One-Dimensional Antiferromagnets, Phys. Rev. Lett. **89**, 047202 (2002).

[8] J. Sirker, S. Fujimoto, N. Laflorencie, S. Eggert, and I. Affleck, Thermodynamics of impurities in the anisotropic Heisenberg spin-1/2 chain, J. Stat. Mech. (2008) P02015.

[9] A. Bohrdt, K. Jägering, S. Eggert, and I. Schneider, Dynamic structure factor in impurity-doped spin chains, Phys. Rev. B **98**, 020402(R) (2018).

[10] M. Jeong, D. Schmidiger, H. Mayaffre, M. Klanjšek, C. Berthier, W. Knafo, G. Ballon, B. Vignolle, S. Krämer, A. Zheludev, and M. Horvatić, Dichotomy between Attractive and Repulsive Tomonaga-Luttinger Liquids in Spin Ladders, Phys. Rev. Lett. **117**, 106402 (2016).

[11] T. Hikihara and A. Furusaki, Spin correlations in the two-leg antiferromagnetic ladder in a magnetic field, Phys. Rev. B **63**, 134438 (2001).

[12] P. Bouillot, C. Kollath, A. M. Läuchli, M. Zvonarev, B. Thielemann, C. Rüegg, E. Orignac, R. Citro, M. Klanjšek, C. Berthier, M. Horvatić, and T. Giamarchi, Statics and dynamics of weakly coupled antiferromagnetic spin-$\frac{1}{2}$ ladders in a magnetic field, Phys. Rev. B **83**, 054407 (2011).

[13] B. R. Patyal, B. L. Scott, and R. D. Willett, Crystal-structure, magnetic-susceptibility, and EPR studies of bis(piperidinium)tetrabromocuprate(II): A novel monomer system showing spin diffusion, Phys. Rev. B **41**, 1657 (1990).

[14] B. Thielemann, C. Rüegg, H. M. Rønnow, A. M. Läuchli, J.-S. Caux, B. Normand, D. Biner, K. W. Krämer, H.-U. Güdel, J. Stahn, K. Habicht, K. Kiefer, M. Boehm, D. F. McMorrow, and J. Mesot, Direct Observation of Magnon Fractionalization in the Quantum Spin Ladder, Phys. Rev. Lett. **102**, 107204 (2009).

[15] B. Thielemann *et al.*, Field-controlled magnetic order in the quantum spin-ladder system $(Hpip)_2CuBr_4$, Phys. Rev. B **79**, 020408(R) (2009); M. Klanjšek, H. Mayaffre, C. Berthier, M. Horvatić, B. Chiari, O. Piovesana, P. Bouillot, C. Kollath, E. Orignac, R. Citro, and T. Giamarchi, Luttinger liquid physics in the spin ladder material $CuBr_4(C_5H_{12}N)_2$, Phys. Status Solidi C **247**, 656 (2010).

[16] D. Schmidiger, P. Bouillot, S. Mühlbauer, S. Gvasaliya, C. Kollath, T. Giamarchi, and A. Zheludev, Spectral and Thermodynamic Properties of a Strong-Leg Quantum Spin Ladder, Phys. Rev. Lett. **108**, 167201 (2012).

[17] A. Shapiro, C. P. Landee, M. M. Turnbull, J. Jornet, M. Deumal, J. J. Novoa, M. A. Robb, and W. Lewis, Synthesis, structure, and magnetic properties of an antiferromagnetic spin-ladder complex: Bis (2, 3-dimethylpyridinium) tetrabromocuprate, J. Am. Chem. Soc. **129**, 952 (2007).

[18] D. Schmidiger, P. Bouillot, T. Guidi, R. Bewley, C. Kollath, T. Giamarchi, and A. Zheludev, Spectrum of a Magnetized Strong-Leg Quantum Spin Ladder, Phys. Rev. Lett. **111**, 107202 (2013).

[19] M. Jeong, H. Mayaffre, C. Berthier, D. Schmidiger, A. Zheludev, and M. Horvatić, Attractive Tomonaga-Luttinger Liquid in a Quantum Spin Ladder, Phys. Rev. Lett. **111**, 106404 (2013); K. Yu. Povarov, D. Schmidiger, N. Reynolds, R. Bewley, and A. Zheludev, Scaling of temporal correlations in an attractive Tomonaga-Luttinger spin liquid, Phys. Rev. B **91**, 020406(R) (2015).

[20] See Supplemental Material at http://link.aps.org/supplemental/10.1103/PhysRevLett.128.237201 for the details of the experiment setup and data analysis, numeric simulations and their interpretation, and the theoretical approach to the finite-size scaling.

[21] B. Bauer, L. D. Carr, H. G. Evertz, A. Feiguin, J. Freire, S. Fuchs, L. Gamper, J. Gukelberger, E. Gull, S. Guertler *et al.*, The ALPS project release 2.0: Open source software for strongly correlated systems, J. Stat. Mech. (2011) P05001.

[22] V. N. Glazkov, M. Fayzullin, Y. Krasnikova, G. Skoblin, D. Schmidiger, S. Mühlbauer, and A. Zheludev, ESR study of the spin ladder with uniform Dzyaloshinskii-Moriya interaction, Phys. Rev. B **92**, 184403 (2015).

[23] D. Schmidiger, K. Yu. Povarov, S. Galeski, N. Reynolds, R. Bewley, T. Guidi, J. Ollivier, and A. Zheludev, Emergent Interacting Spin Islands in a Depleted Strong-Leg Heisenberg Ladder, Phys. Rev. Lett. **116**, 257203 (2016).

[24] H.-J. Mikeska, U. Neugebauer, and U. Schollwöck, Spin ladders with nonmagnetic impurities, Phys. Rev. B **55**, 2955 (1997); M. Sigrist and A. Furusaki, Low-temperature properties of the randomly depleted Heisenberg ladder, J. Phys. Soc. Jpn. **65**, 2385 (1996); A. Lavarélo, G. Roux, and N. Laflorencie, Magnetic responses of randomly depleted spin ladders, Phys. Rev. B **88**, 134420 (2013).

[25] M. Kenzelmann, G. Xu, I. A. Zaliznyak, C. Broholm, J. F. DiTusa, G. Aeppli, T. Ito, K. Oka, and H. Takagi, Structure of End States for a Haldane Spin Chain, Phys. Rev. Lett. **90**, 087202 (2003).

[26] J. Ollivier and H. Mutka, IN5 cold neutron time-of-flight spectrometer, prepared to tackle single crystal spectroscopy, J. Phys. Soc. Jpn. **80**, SB003 (2011).

[27] R. A. Ewings, A. Buts, M. D. Le, J. van Duijn, I. Bustinduy, and T. G. Perring, HORACE: Software for the analysis of data from single crystal spectroscopy experiments at time-of-flight neutron instruments, Nucl. Instrum. Methods Phys. Res., Sect. A **834**, 132 (2016).

[28] D. Blosser, V. K. Bhartiya, D. J. Voneshen, and A. Zheludev, $z = 2$ Quantum Critical Dynamics in a Spin Ladder, Phys. Rev. Lett. **121**, 247201 (2018); Origin of magnetic anisotropy in the spin ladder compound $(C_5H_{12}N)_2CuBr_4$, Phys. Rev. B **100**, 144406 (2019).

[29] M. Reigrotzki, H. Tsunetsugu, and T. M. Rice, Strong-coupling expansions for antiferromagnetic Heisenberg spin-one-half ladders, J. Phys. Condens. Matter **6**, 9235 (1994).

[30] T. Giamarchi and A. M. Tsvelik, Coupled ladders in a magnetic field, Phys. Rev. B **59**, 11398 (1999).

[31] A. W. Sandvik, Stochastic series expansion method with operator-loop update, Phys. Rev. B **59**, R14157 (1999); F. Alet, S. Wessel, and M. Troyer, Generalized directed loop method for quantum Monte Carlo simulations, Phys. Rev. E **71**, 036706 (2005).

[32] H. J. Schulz, Dynamics of Coupled Quantum Spin Chains, Phys. Rev. Lett. **77**, 2790 (1996).

[33] C. Yasuda, S. Todo, K. Hukushima, F. Alet, M. Keller, M. Troyer, and H. Takayama, Néel Temperature of Quasi-Low-Dimensional Heisenberg Antiferromagnets, Phys. Rev. Lett. **94**, 217201 (2005).

[34] K. Trinh and S. Haas, Bond disorder in even-leg Heisenberg ladders, Phys. Rev. B **87**, 075137 (2013).
[35] E. Wulf, S. Mühlbauer, T. Yankova, and A. Zheludev, Disorder instability of the magnon condensate in a frustrated spin ladder, Phys. Rev. B **84**, 174414 (2011).
[36] C. L. Kane and M. P. A. Fisher, Transport in a One-Channel Luttinger Liquid, Phys. Rev. Lett. **68**, 1220 (1992).
[37] G. Blumberg, P. Littlewood, A. Gozar, B. S. Dennis, N. Motoyama, H. Eisaki, and S. Uchida, Sliding density wave in $sr_{14}cu_{24}o_{41}$ ladder compounds, Science **297**, 584 (2002); S. Sahling, G. Remenyi, C. Paulsen, P. Monceau, V. Saligrama, C. Marin, A. Revcolevschi, L. P. Regnault, S. Raymond, and J. E. Lorenzo, Experimental realization of long-distance entanglement between spins in antiferromagnetic quantum spin chains, Nat. Phys. **11**, 255 (2015).
[38] H. Takahashi, A. Sugimoto, Y. Nambu, T. Yamauchi, Y. Hirata, T. Kawakami, M. Avdeev, K. Matsubayashi, F. Du, C. Kawashima, H. Soeda, S. Nakano, Y. Uwatoko, Y. Ueda, T. J. Sato, and K. Ohgushi, Pressure-induced superconductivity in the iron-based ladder material $BaFe_2S_3$, Nat. Mater. **14**, 1008 (2015); Y. Hirata, S. Maki, J.-i. Yamaura, T. Yamauchi, and K. Ohgushi, Effects of stoichiometry and substitution in quasi-one-dimensional iron chalcogenide $BaFe_2S_3$, Phys. Rev. B **92**, 205109 (2015).